Polycyclic aromatic hydrocarbon compound excursions and K/Pg transition in the late Cretaceous–early Palaeogene succession of the Um Sohryngkew river section, Meghalaya

Sucharita Pal[1], J. P. Shrivastava[1,*] and Sanjay K. Mukhopadhyay[2]

[1]Department of Geology, University of Delhi, Delhi 110 007, India
[2]Plot No. 2, Nabaroon Co-Op. Housing Society, Santoshree Palli, Thakurpukur, Kolkata 700 063, India

A combustion-derived polycyclic aromatic hydrocarbon (PAH) compounds based high-resolution stratigraphic records across the Cretaceous/Palaeogene boundary section of the Um Sohryngkew river section is presented in this paper. The yellowish brown, organic-rich, 1 to 2 mm thick, clay layer in biozone CF3 is marked by sudden increase in the high molecular weight fluoranthene, pyrene, chrysene, benzo(a) anthracene PAH compounds. These componds are similar to those associated with the well-known K/Pg boundary sections across the world. Besides these, high abundance of low molecular weight 3 ring anthracene and fluorine, and 4 ring PAH compounds is also noticed in this layer. Subordinate amount of low molecular weight 3-ring phenanthrene, 3-methylphenanthrene, 2-methylphenanthrene, 9-methylphenanthrene and 1-methylphenanthrene PAH compounds have also been found in the successive layer of biozone CF2. Occurrence of high molecular weight PAH compounds in the biozone CF3 (66.83–65.45 Ma age) imply global fire, induced by the heat supplied by Abor/Deccan volcanic activity, possibly linked with the K/Pg boundary transition events as later initiated prior to the K/Pg boundary, however, the main episode of Deccan volcanic activity occurred ~300 ky earlier or at the K/Pg boundary itself. PAH compound anomalies in the biozone CF3 is well coinciding with the well documented Ce anomaly layer, but, preceded by planktonic foraminiferal break and PGE anomaly bearing layer in the biozone P0. It is inferred that the K/Pg boundary related global fire played significant role in the collapse of the ecosystem, causing sudden demise of organisms.

Keywords: Organo-molecules, polycyclic aromatic hydrocarbon compounds, stratigraphic record, volcanic activity.

ORGANIC matter associated with the sedimentary rocks contains chemically complex and geologically stable organic molecules that help in the palaeoenvironmental reconstruction[1]. Fossilized organic molecules in the K/Pg boundary sediments provide useful information about mass extinction. An earlier study on organic matter associated with iridium-enriched Anjar intertrappean layer marked the presence of aliphatic compounds[2]. Association of Ir anomalies with the basal coal layer at the K/Pg boundary site of Raton in Colorado[3], soot layers of boundary sites[4,5], and spikes in the abundances of polycyclic aromatic hydrocarbon (PAH) compounds at the K/Pg boundary in Caravaca, Spain[6], presented evidence of global fires during the boundary event. Thus, fossilized PAH compounds derived from higher plant detritus and degradation products remain less affected or unchanged by geological processes and are significant in this context.

Despite the presence of late Cretaceous and early Palaeogene marine strata[7] as well as Deccan Traps and associated sedimentary successions[8–11], the Indian subcontinent is not known to have a Cretaceous/Palaeogene (K/Pg) boundary section comparable to international standards. Therefore, precise identification of boundary events and their bearing on the palaeogeography and palaeoclimate remained inconclusive until an uninterrupted, finely resolved, shallow marine section (Figure 1) from Meghalaya was discovered[12]. It is located on the west bank of the Um Sohryngkew river, where late Maastrichtian–early Danian sequence constitutes the lowermost part of a continuous marine section, ranging from late Cretaceous through early Oligocene. The high-resolution stratigraphy (based on planktonic foraminiferal zones) indicates that the Um Sohryngkew river section is continuous across the boundary[13]. The contentious issues related to the position of K/Pg boundary layer (Figure 2) (ref. 14) and references therein), geochemical anomalies and foraminiferal changes were reviewed and based on total organic compound (TOC), δCe and δEu values, assigned suboxic/anoxic – suboxic – suboxic/anoxic–oxic conditions for bottom sea-water sediments (from biozone CF4 to Pla). These layers in ocean sediments largely correspond to the planktonic foraminiferal extinction[12], and Au, Pt and Pd anomalies[13]. Since the zonal indices of the late Maastrichtian zones are sparse in the studied sections

*For correspondence. (e-mail: jpshrivastava.du@gmail.com)

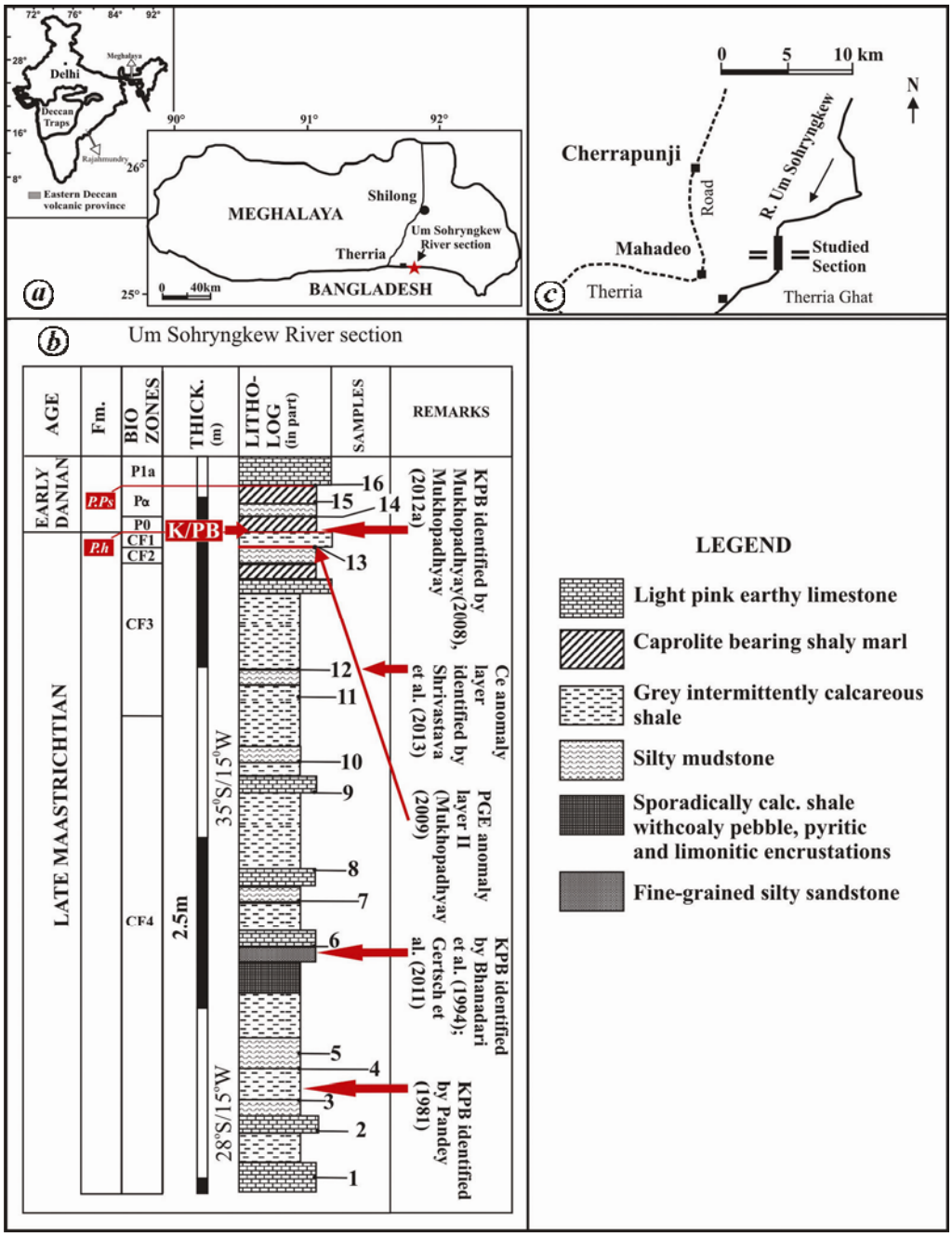

Figure 1. Lithostratigraphy (modified after ref. 12) and sample locations on the Um Sohryngkew river section. ***a***, Location of Meghalaya with respect to India. ***b***, Location of the Therriaghat section around the Um Sohryngkew river. ***c***, Lithological log at the K/Pg interval in the Um Sohryngkew river section. Note: Samples 1–16 collected from the section are referred to as JP1–JP16 in the text.

and often occur in association with reworked forms, the boundaries of the CF zones are tentative. Thus, it is necessary to understand the nature and abundance of organic macromolecular PAH compounds in this succession to comprehend palaeoenvironmental reasons accountable for their derivation from the original organic source matter at the end of the Cretaceous period. Recognition as well as variation in the distribution of PAH molecules, if recorded across the succession, would unveil palaeoenvironmental variables accountable for their derivation. However, such studies have not been carried out in this area. The present article aims to record variation in the organic molecules across the succession. The correspondence between macroorganic anomalies and the K/Pg boundary events is also attempted.

According to the sample sites marked (black solid circles in Figure 1 *c*) in the mapped litholog, samples JP1–JP16 were collected from the middle part of the Langpar

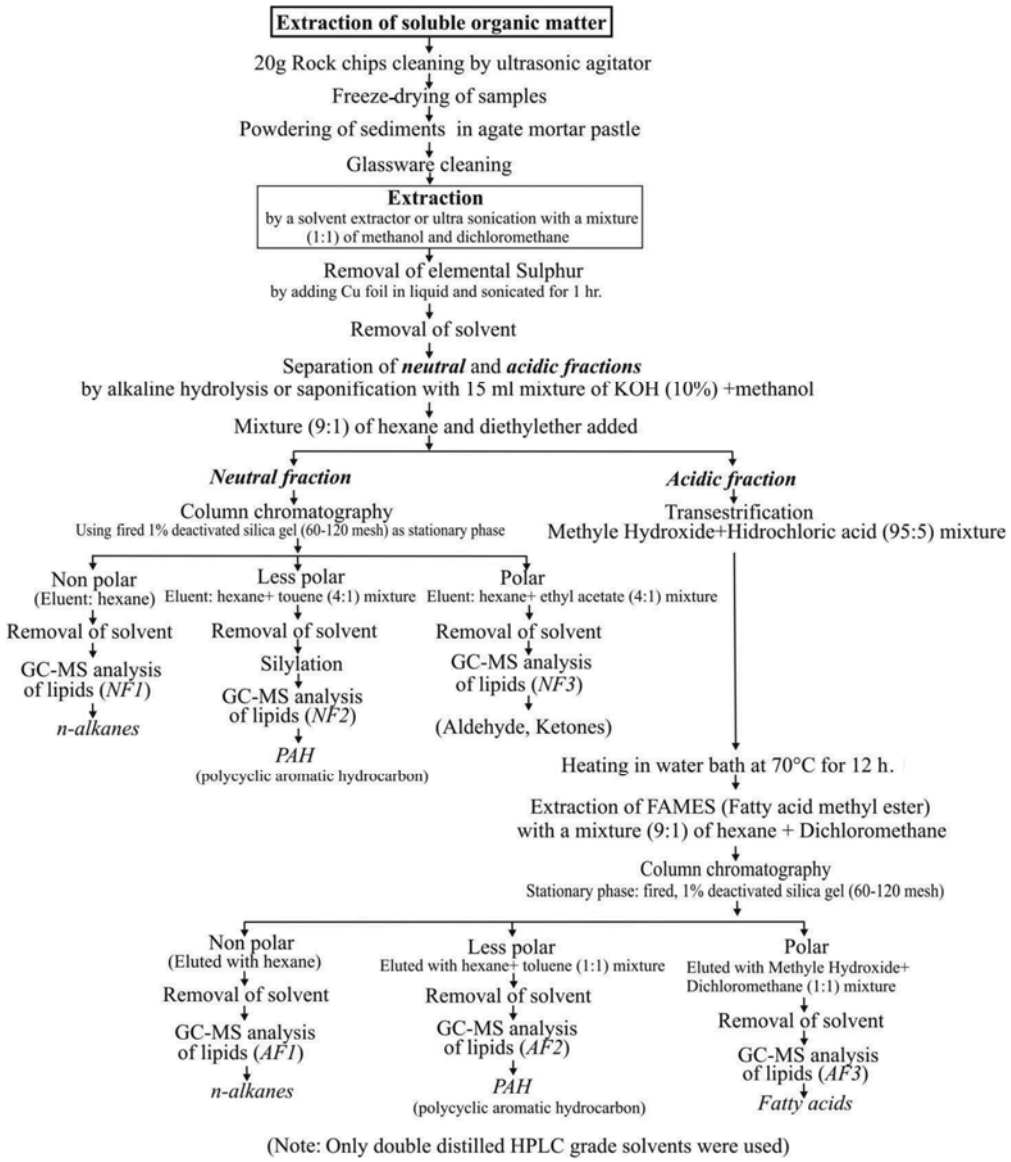

Figure 2. Summary of the mechanical and chemical procedures (modified after refs 6, 15, 16) used in the extraction of soluble organic matter.

Formation, covering the K/Pg boundary. Each sample of 50–70 g was collected from 25 cm below the surface. For friable sediments, hollow steel pipe (3.5 cm diameter with one end pointed) was used as an auger to avoid contamination. Samples were broken into small pieces (2–4 mm) with a steel hammer. Approximately 20 g sample chips were cleaned twice by ultrasonic agitation with a solvent mixture of benzene and methanol (6 : 4) for 5 min and allowed to freeze-dry, and finally powdered using agate pestle mortar to pass through 200 mm mesh sieve. For gas chromatography–mass spectroscopy (GC–MS), a combination of mechanical and chemical procedures[6,15,16] was employed (Figure 2). Samples (15 g) were extracted three times with a solvent mixture of methanol and dichloromethane (1 : 1) by a solvent extractor with ~80% recovery. After removing elemental S (by adding Cu foil and sonication for 1 h), 15 ml of (10%) KOH–methanol solution and 2 ml water were added to the 10 ml extract. The extracts were fractionated into neutral (NF) and acidic (AF) compounds (by liquid–liquid separation) by dissolving in *n*-hexane + diethyl ether (9 : 1) and *n*-hexane + dichloromethane (9 : 1) mixtures respectively. Neutral compounds were fractionated into aliphatic hydrocarbons, PAH compounds, and other group compounds using silica-gel (heated at 200°C, 1% deactivated) column [borosilicate glass column size – 100 cm (length) and 0.8 mm (internal diameter)] chromatography.

After methylation, 15 ml MeOH : HCl (95 : 5) mixture was added to AF. After heating gently in the water bath at 70°C for 12 h, acid will form methyl ester or diazonium

salt (according to the derivatizing agent). Boron triflouride forms a complex with methanol and it reacts with an acid and active hydrogen from the acid (–OH) is replaced by methyl group, forming a methyl ester. For extraction of fatty acids, 0.5 ml of 2 mg methyl ester standard solution prepared in 100 cc dichloromethane was poured by a syringe in the AF. FAMES (fatty acid methyl ester) was extracted from acidic compounds with a *n*-hexane and diethyl ether solvent mixture (9 : 1). Acidic compounds were fractionated into fatty acids and the remaining aliphatic hydrocarbons and PAH compounds by silica-gel column chromatography. The PAH compounds were analysed using gas chromatograph (GC-2010) and mass spectrometer (QP2010) with a Shimadzu AOC-20i auto sampler. A 20 m × 0.1 mm id (0.1 μm film thickness) fused silica capillary column (RTX-5) was used. The carrier gas used was helium (0.1 ml/min). The injector and detector temperatures were set at 250°C and 220°C respectively. The oven temperature programme was – 1 min hold at 50°C; ramp to 10°C at 140°C/min, and ramp to 6°C at 320°C/min and 5 min hold. The PAH compounds were identified by comparing the retention time with the PAH Mix standards (procured from National Institute of Standards and Technology Spectral Reference Library) within a range ± 0.1 min and particular ratios of several relatively abundant ions. The analysis was performed in electron ionization (EI) SIM mode at 70 eV. Absolute quantification method with external standards was used for quantification of individual compounds. Analytical uncertainty is expressed as RSE%, which is 30.6% for the present analysis. Ratio of signal/noise (S/N) = 10 was considered as quality norms for analysis of all PAH compounds. Any value less than that is below the limit of detection. Thus the detection limit of data is <0.01 μg/g TOC.

The PAH compounds were monitored for dibenzothiophine (*m*/*z*-146), phenanthrene (*m*/*z*-178), 3-methylphenanthrene (*m*/*z*-192), 2-methylphenanthrene (*m*/*z*-912), 9-methylphenanthrene (*m*/*z*-192), 1-methylphenanthrene (*m*/*z*-192), 2-methylanthracene (*m*/*z*-192), fluoranthene (*m*/*z*-202), pyrene, (*m*/*z*-202), 1-methyl pyrene (*m*/*z*-216), chrysene (*m*/*z*-228), benzo(k)fluoranthene (*m*/*z*-252), benzo(e)pyrene (m/z-252) and benzo(a)pyrene (*m*/*z*-252). The absolute quantification method with external standard (EPA 16 PAH) was employed for quantification of individual compounds. Relative standard deviation of the individual alkanes and PAH compound concentrations were <10% and 15% respectively. The validation method consists of five sets of samples. Each set consists of four different concentrations (e.g. 2, 4, 6, 8 ppb) and a blank. All the 20 samples were processed similarly and concentrations were calculated. From the standard and observed values, the percentage recovery was calculated (using the formula percentage recovery = observed value/true value × 100).

The initial extractable concentration of 20 non-volatile PAH compounds was 524.67 μg/g TOC sediments. Total PAH concentration varied between 1.20 and 109.74 μg/g TOC (Table 1). The spectra (Figure 3) obtained for the samples show the presence of 20 lipophilic PAH compounds which consist of 2–5 benzene rings. Among these, the chief PAH compounds present in the succession were phenanthrene, fluorene, fluoranthene and pyrene. The 3-, 4-, 5- and 6-ring PAH compounds represent 32%, 28%, 29% and 9% of the total extractable PAH compounds respectively. Based on the number of rings present in the PAH compound structures, they have been grouped into (i) lower molecular weight (LMW) PAH compounds, containing 2–4 rings, and (ii) higher molecular weight (HMW) PAH compounds, containing 5–7 rings[17]. Samples JP-2, JP-5, JP-9, JP-11, JP-13 and JP-14 show high amount of LMW (2–3 ring PAH compounds), whereas JP-1, JP-6–8, JP-10, JP-12, JP-15 and JP-16 show high amount of HMW (4–5 ring PAH compounds). Distribution of PAH compounds and their ratios helps distinguish such compounds of petrogenic and pyrolytic origin. For source recognition of PAH compounds, two diagnostic ratios: (i) benzo[a]anthracene/benzo[a]anthracene + chrysene (BaA/BaA + Cry) and (ii) fluoranthene/fluoranthene + pyrene (Fl/Fl + Py) were used for the present work, where the main concern was to select ratios based on compounds (above detection limit) present in most of the samples and determined by molecular ratios of some of the PAH compounds[18,19]. Pyrogenic ratio[20] was calculated by dividing sum of the 3–6 ring PAH compounds (excluding non-alkylated homologues in five alkylated series) by the sum of five alkylated series (naphthalenes, fluorenes, phenanthrenes, chrysenes and dibenzothiophenes) (Table 1).

PAH concentrations when plotted across the succession (Figure 4 *a* and *b*) show dominance of LMW compounds in the biozone CF1 (sample JP-13), while HMW compounds predominate in the biozone CF3 (sample JP-12). For these samples, the ratio of LMW and HMW PAH compounds is applied for source discrimination as their values lower than unity indicate pyrogenic origin, while values 2–6 indicate petrogenic input into the marine environment. Pyrogenic PAH compounds are characterized by high abundance of HMW and unsubstituted compounds, whereas petrogenic PAH compounds are dominated by alkyl-substituted as well as LMW compounds[18]. PAH compounds of 4 and 5 benzene rings present in the section were produced by the microbial breakdown of plant wax and woody tissues, suggestive of faster degradation of PAH compounds that enter into the marine sediments[21]. The high PAH compound values are not related to high TOC, indicative of soot particles associated with the sediments coming from atmospheric transportations. Phenanthrene is the most important compound in the alkylated series. Maximum concentration (8.28 and 5.72 μg/g TOC) of phenanthrene and chrysene was noticed in biozones CF3 (sample JP-12) and CF1 (sample JP-13), formed during diagenesis as biological precursors[22].

Table 1. Concentrations (μg/g TOC) of polycyclic aromatic hydrocarbons (PAH) compounds obtained from GC–MS analysis and their calculated parameters for JP-1 to JP-16 samples collected from Um Sohryngkew river section

PAH compounds (μg/g TOC)	Samples															
	JP-1	JP-2	JP-3	JP-4	JP-5	JP-6	JP-7	JP-8	JP-9	JP-10	JP-11	JP-12	JP-13	JP-14	JP-15	JP-16
Napthalene	–	–	–	–	–	–	–	1.14	–	1.59	–	0.08	6.90	0.27	0.16	0.02
Acenapthylene	–	–	–	–	–	–	–	0.05	–	0.02	–	0.01	0.03	–	0.03	0.05
Accnapthene	–	–	–	–	–	–	–	0.05	–	0.02	–	0.03	–	–	0.01	0.02
Fluorene	0.20	–	0.01	–	–	0.04	–	0.39	–	0.52	–	1.49	0.15	0.15	0.52	0.66
Phenanthrene	0.17	0.32	0.29	0.63	0.92	0.21	–	0.87	0.11	0.80	0.49	1.33	5.72	2.32	0.93	0.48
Anthracene	6.36	0.42	0.32	0.81	1.49	2.46	0.11	16.79	0.09	13.68	0.75	22.96	7.11	3.42	15.15	17.69
Fluoranthrene	4.27	0.34	0.16	0.41	0.48	0.52	0.25	6.70	0.09	5.07	0.46	10.46	1.62	1.16	4.86	7.57
Pyrene	3.17	0.34	0.12	0.34	0.75	0.90	0.22	5.44	0.09	4.51	0.33	7.20	2.18	1.28	5.61	6.00
1-Methylanthracene	0.06	0.12	0.11	0.32	0.56	0.14	–	0.30	0.04	0.28	0.12	0.56	2.08	1.26	0.56	0.17
1-Methylphenanthrene	0.07	0.16	0.15	0.38	0.68	0.21	–	0.45	0.05	0.35	0.15	0.76	2.85	1.60	0.78	0.23
Chrysone	1.34	0.16	0.12	0.13	0.26	0.31	0.07	4.16	0.04	2.90	0.18	8.28	0.65	0.68	3.65	3.60
Benzo(a)anthracene	3.92	0.26	0.15	0.25	0.55	0.40	0.11	5.61	0.07	4.02	0.31	9.92	1.06	1.04	4.53	6.91
2-Methylphenanthrene	0.17	0.32	0.29	0.63	0.92	0.21	–	0.87	0.11	0.80	0.49	1.33	5.72	2.32	0.93	0.48
9-Methylphenanthrene	0.08	0.16	0.15	0.44	0.78	0.19	–	0.41	0.05	0.35	0.16	0.72	2.89	1.63	0.70	0.26
3-Methylphenanthrene	–	0.03	–	0.04	0.09	0.06	–	0.07	0.01	0.11	0.04	0.20	–	0.50	0.19	0.02
Benzo(k)fluoranthene	6.60	0.11	0.25	0.13	0.58	0.44	–	8.54	0.13	7.20	0.30	13.04	1.68	1.52	6.75	8.77
Benzo(a)fluoranthene	7.70	0.32	0.29	0.31	0.70	0.52	0.32	9.87	0.15	8.35	0.55	15.13	1.98	1.78	7.85	10.17
Benzo(a)pyrene	0.58	0.16	0.12	0.09	0.12	0.33	–	3.92	0.02	2.96	0.14	6.04	0.62	0.65	3.78	1.88
Indeno(1,2,3-cd)pyrene	3.08	0.40	0.27	0.19	0.60	0.65	0.22	7.33	0.15	5.75	0.37	7.95	1.56	2.20	6.94	6.86
Dibenzo(a,b)anthracene	0.64	0.03	0.02	0.03	0.07	0.04	–	1.16	–	1.09	0.05	2.25	0.12	0.24	1.28	1.22
Calculated parameters																
Total PAH	38.42	3.64	2.81	5.13	9.56	7.62	1.30	74.12	1.20	60.38	4.89	109.74	44.94	24.02	65.22	73.05
LMW/HMW	0.23	0.71	0.87	1.71	1.30	0.84	0.09	0.40	0.75	0.44	0.80	0.36	2.92	1.23	0.44	0.38
Fl/Py	1.348	1	1.333	1.181	0.645	0.581	1.166	1.231	1	1.123	1.416	1.453	0.743	0.906	0.866	1.260
Ph/An	0.027	0.75	0.903	0.769	0.612	0.084	–	0.051	1.25	0.058	0.654	0.057	0.804	0.678	0.061	0.026
Mp/P	–	2.215	5.666	5.136	3.942	0.835	–	0.373	2.789	0.396	2.792	0.468	6.203	5.324	0.530	0.189
Fl/(Fl + Py)	0.57	0.50	0.57	0.54	0.39	0.37	0.54	0.55	0.50	0.53	0.59	0.59	0.43	0.48	0.46	0.56
Ba/(Ba + Chry)	0.75	0.63	0.56	0.67	0.68	0.56	0.60	0.57	0.60	0.58	0.64	0.55	0.62	0.60	0.55	0.66
3-5 ring/5alkylated PAH	20.61	6.77	6.07	6.52	7.51	12.29	15.00	10.18	6.74	9.39	6.69	9.09	3.23	6.23	11.05	13.91
3-6 ring/5alkylated PAH	22.41	7.60	6.71	6.77	8.02	13.44	18.00	11.30	7.74	10.38	7.24	9.80	3.35	6.88	12.38	15.35

LMW/HMW, Low molecular weight/high molecular weight; Fl, Fluoranthene; Py, Pyrene; Ph, Phenanthrene; An, Anthracene; MP, ∑(3-methylphenanthrene, 2-methylphenanthrene, 9-methylphenanthrene, 1-methylphenanthrene); BA, Benzo(a)anthracene; chry, Chrysene; 3–5 ring/5 alkylated PAH, [∑(anthracene, fluorene, phenanthrene, 3-methylphenanthrene, 2-methylphenanthrene, 9-methylphenanthrene, 1-methylphenanthrene fluoranthene, benzo(a)anthracene, chrysene, pyrene, benzo(a)fluoranthene, benzo(k)fluoranthene, benzo(a)pyrene, dibenzo(a,b)anthracene)/ ∑naphthalene, fluorene, phenanthrene, phenanthrene], 3-6 ring/5 alkylated PAH, [∑(anthracene, fluorene, phenanthrene, 3-methylphenanthrene, 2-methylphenanthrene, 9-methylphenanthrene, 1-methylphenanthrene fluoranthene, benzo(a)anthracene, chrysene, pyrene, benzo(a)fluoranthene, benzo(k)fluoranthene, benzo(a)pyrene, dibenzo(a,b)anthracene)indeno (1,2,3-c,d) pyrene/∑ naphthalene, fluorene, phenanthrene, phenanthrene]; (–), Below the limit of detection, i.e. < 0.01 μg/g TOC.

Phenanthrene (<0.01–5.72 μg/g TOC) and its methylated homologues (9-methylphenanthrene) represent similar patterns and concentrations (i.e. <0.01–2.85 μg/g TOC) as their maximum concentrations were recorded from the late Maastrichtian biozone CF1 (Figure 4 *a*, sample JP-13). Exceptionally, high amount of benzo[a]anthracene (9.92 μg/g TOC), fluoranthene (10.46 μg/g TOC) and pyrene (7.20 μg/g TOC) is associated with the sample JP-12 of biozone CF3, signify almost similar trends (Figure 4 *b*), thus, originated from similar source. It has been established that benzo[a]anthracene, fluoranthene, and pyrene are combustion-derived components, resulting from palaeo forest fires[23]. The Fl/(Fl + Py) values vary between 0.37 and 0.59 and BaA/(BaA + Cry) > 0.35 in these samples (JP1-16), suggestive of combustion of organic matter trapped within the sediments[19]. Pyrolytic and petrogenic zones were distinguished when fluoranthene/pyrene (Fl/Py) versus phenanthrene/anthracene (P/A) and methylphenanathrene/phenanthrene (MP/P) values were plotted (Figure 5 *a* and *b*), indicating that 11 data plots clustered within the pyrolitic field, whereas the remaining 5 data plots lay within the petrogenic field. However, data plots for JP-2 and JP-9 fall on the margin between pyrolytic and petrogenic fields. The fluoranthrene/pyrene (F/P) values >1 signify pyrolytic source, whereas F/P <1 indicates petroleum hydrocarbon source[24]. Similarly, P/A values <10 indicate combustion source and value >10 indicates petrogenic source[25]. Present F/P and P/A values (Table 1) obtained for JP1-16 samples vary between 0.58 and 1.45 and <0.01 and 1.25 respectively, suggesting pyrolytic origin. The 3–5-ring PAH/5 alkylated series considered (as the present

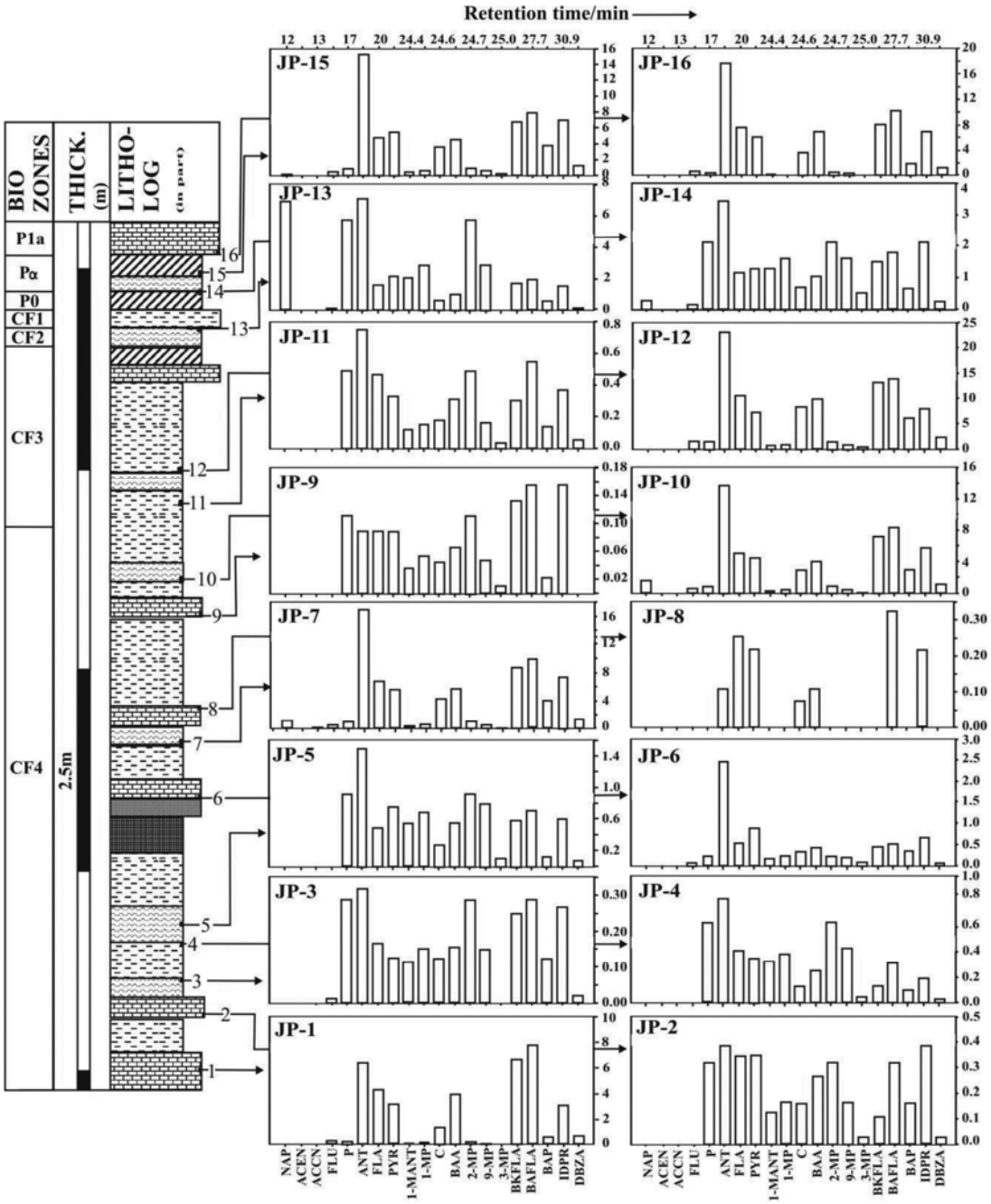

Figure 3. GC–MS spectra of polycyclic aromatic hydrocabon (PAH) compounds arranged in stratigraphic order (1–16). PAH distribution across the Um Sohryngkew river K/Pg boundary succession based on compounds identified by their spectral peaks. The following compounds in the external standard mixtures were quantified: naphthalene (NAP), acenapthylene (ACEN), accnapthene (ACCN), fluorene (FLU), phenanthrene (P), anthracene (ANT), fluoranthene (FLA), pyrene (PYR), 1-methylanthracene (1-MANT), 1-methylphenanthrene (1-MP), chrysene (C), benzo(a)anthracene (BAA), 2-methylphenanthrene (2-MP), 9-methylphenanthrene (9-MP), 3-methylphenanthrene (3-MP), benzo(k)fluoranthene (BKFLA), benzo(a)fluoranthene (BAFLA), benzo(a)pyrene (BAPYR), indeno (1,2,3-c,d) pyrene (IDPR) and dibenzo(a, b)anthracene (DBZA). Legend: same as in Figure 1.

samples do not contain 6-ring PAH compounds) in the present study show values >0.8, suggestive of pyrogenic source[24,25].

When the PAH compound data of biozone CF3 were compared with the combustion marker PAH compounds of the K/Pg boundary sections of Stevns Klint (Denmark), Gubbio (Italy) and Woodside Creek (New Zealand), their values showed excursions (Figure 6) and represented the K/Pg boundary layer. Such type of environment was possibly created in the interspaces of the sediments by burning of organic matter in the presence of oxygen, thus forming CO_2 and water. Interestingly,

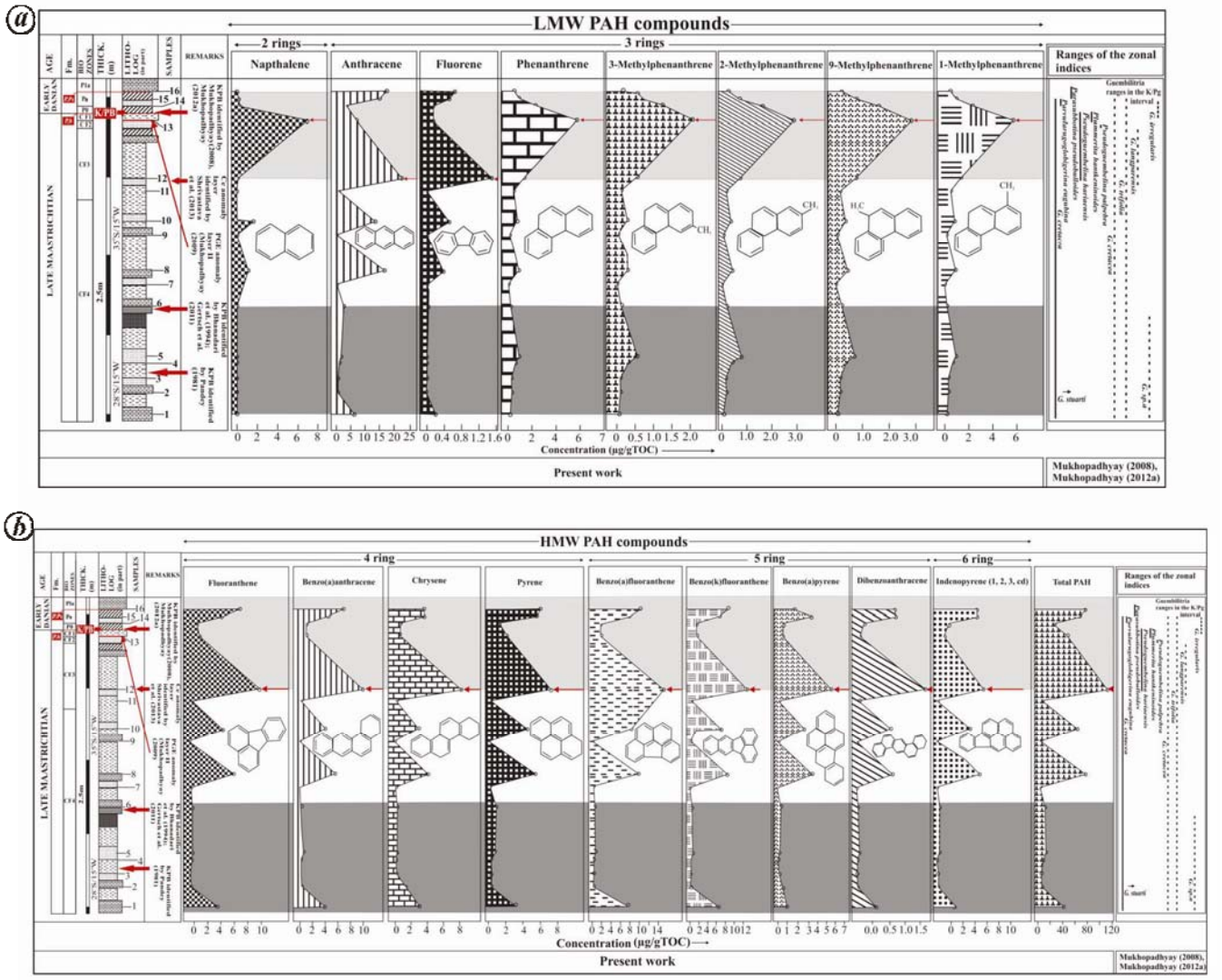

Figure 4. ***a***, Um Sohryngkew river stratigraphic log showing sequential changes in the low molecular weight (LMW) PAH compounds. Excursions of naphthalene, anthracene, fluorene, phenanthrene, 3-methylphenanthrene, 2-methylphenanthrene, 9-methylphenanthrene, 1-methylphenanthrene are shown with red arrows (←). 2, 3 benzene rings are shown within their respective columns. ***b***, Um Sohryngkew stratigraphic log showing sequential changes in the high molecular weight (HMW) PAH compounds and calculated parameters. Excursions of fluoranthene, benzo(a)anthracene, chrysene, pyrene, benzo(a)fluoranthene, benzo(k)fluoranthene, benzo(a)pyrene, dibenzo(a,b)anthracene, indeno(1,2,3-c,d) pyrene and total PAH compounds are shown with red arrows (←).4–6 benzene rings are shown within their respective columns. LMW, low molecular weight; HMW, high molecular weight.

enhanced phenanthrene, anthracene, pyrene and fluoranthene concentrations were also reported[26] from K/Pg boundary sections of Stevns Klint (Denmark), Gubbio (Italy) and Woodside Creek (New Zealand), suggesting that such molecular structures were derived from global fires associated with the K/Pg mass extinction event. Comprehensive studies on the distribution of PAH compounds (in the Upper Jurassic sediments) suggest that the periodic wild fires were the main source of PAH compounds containing three or more aromatic rings[22].

Incomplete combustion of organic matter is the most important source for unsubstituted PAH (fluoranthene, pyrene, benzo[a]anthracene, benzo[b]fluoranthene, benzo[k]fluoranthene, benzo[e]pyrene, benzo[a]pyrene) compounds. Thus, phenanthrene-12 and chrysene-13 originated from the combustion and diagenetic processes of organic matter (OM)[27]. HMW fraction of PAH compounds produced by biomass burning was most likely moved through the atmosphere into aquatic environments, however, with little change in the composition. Palaeo-fires are likely to be an important source of pyrolytic PAH compounds and perhaps a characteristic of terrestrial ecosystems. The heat required for the formation of PAH compounds in the sedimentary environments was possibly supplied by the contemporaneous Abor[28,29] or Deccan volcanic activity[8,10] that occurred in the Indian subcontinent and or collision between Indian and Eurasian plates (66 Ma)[30].

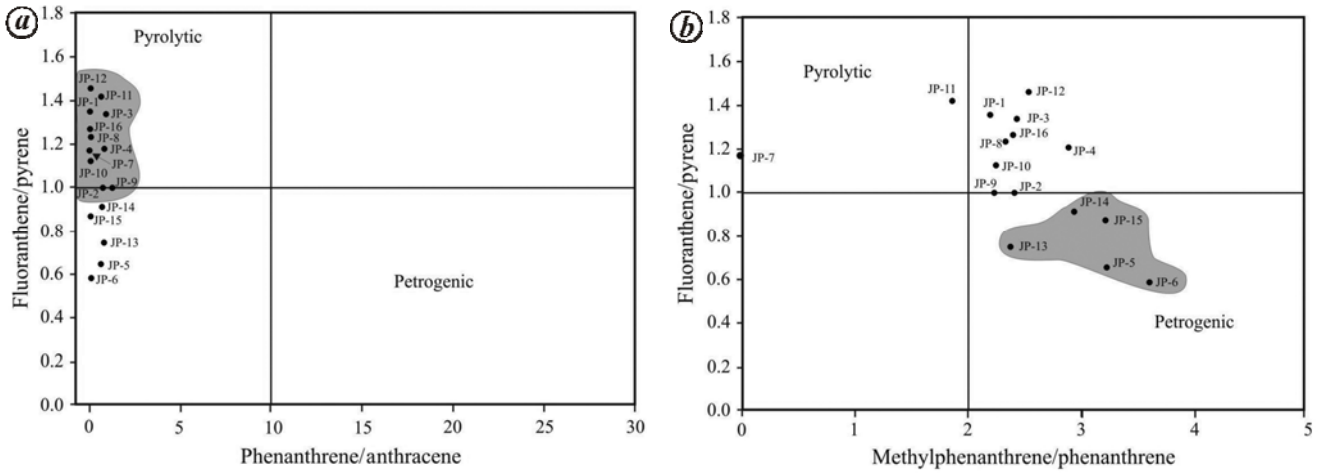

Figure 5. Binary diagram of (***a***) Fl/Py versus Ph/An and (***b***) Fl/Py versus MP/P ratios showing 11 data plots clustered together (shown with grey field) in pyrolytic field (***a***) and (***b***) five data plots lie within the petrogenetic field (shown with grey colour).

The pyrolytic PAH compounds (characterized by the dominance of non-alkylated molecules), especially highly pericondensed compounds (such as compact structures of pyrene and benzopyrene) present in the succession resulted from extensive angular fusion. Such compounds form under-depleted oxygen conditions by the action of heat and result from combustion process; therefore, they are pyrolytic products. The pericondensed PAH compound structures are more reactive than their angularly condensed analogues, and their high concentration among pyrolytic products is ascribed to rapid quenching by adsorption (through hydrogen bonding) onto the soot particles[26]. The K/Pg fires were of high intensity (800°C) and destroyed any amount of charcoal that was produced[31]. However, the charcoal so created persisted up to 1000°C temperatures and even delicate charred plant parts (e.g. moss) remained unaffected combustion in an ambient O_2 conditions[2] at temperatures of ~800°C. The relative concentration of individual PAH compounds is linked with the intensity of the wildfire as well as the type of organic influx[32]. Increasing number of hydrocarbon rings within the compound reflects an increased temperature of formation. Dominance of 2–3-ringed forms in the succession is consistent with the low-moderate intensity fires, whereas high-intensity fires produce elevated concentrations of 5–6-ringed forms[32]. It has been noticed that fluorene and phenanthrene are dominantly present in all the samples and both these forms possess three-ringed aromatic structures. Limited abundance of five-ringed forms is observed; however, no quantifiable levels of six-ringed forms have been observed. Lack of HMW PAH compounds argues against high temperatures of formation, argues against high intensity charcoal destructive K/Pg wildfires[33]. Combustion-derived PAH compounds are abundant in the succession and show distinct distribution (biozone CF3 is marked by high abundance compared to the lower and upper biozones) patterns. The episode of Deccan volcanic activity of a short time span[34], straddling the Cretaceous–Palaeogene boundary (66 Ma)[35] was accountable for the high abundance of these components in JP-12. The distance between sources of the combustion-derived PAH compounds to marine depositional environment and diverse timing of local forest-fire events are accountable for variations in these PAH compounds. Most of the PAH compounds such as pyrene, fluoranthene, benzo[a]anthracene, benzo(a)fluoranthenes, benzo[a]pyrene are ascribed to combustion-derived sources, and show high concentrations either immediately before or shortly after the main extinction events in the section (sample JP-12). While comparing individual compounds of the present section with well-known worldwide K/Pg boundary sections of Gubbio (Italy), Stevens Klint (Denmark) and Woodsite Creek (New Zealand) (Figure 6), it has been found that the present section contains almost all (0.05%–42%) the compounds, but comparatively in a much higher proportion. Pyrosynthetic PAH compounds mainly of non-alkylated species were reported[26] from the K/Pg boundary clays from Gubbio (Italy), Stevans klint (Denmark) and Woodside Creek (New Zealand). The biostratigraphically well-defined K/Pg boundaries at Arroyo el Mimbral, Tamaulipas, Mexico are marked by the presence of fluoranthene, pyrene, chrysene, benzoanthracene and several penta-aromatic compounds[36]. Interestingly, very high concentrations (10.46 μg/g TOC, 7.20 μg/g TOC, 8.28 μg/g TOC, 9.92 μg/g TOC) of these compounds (fluoranthene, pyrene, chrysene, benzoanthracene) were recognized in biozone CF3 (sample JP-12) which lies below biozone P0 (signifying planktonic foraminiferal break) and PGE anomaly-bearing layer[12,13] (Figure 4 *a* and *b*).

PAH compound excursions in biozone CF3 are due to regional fire event which occurred during biozone CF3

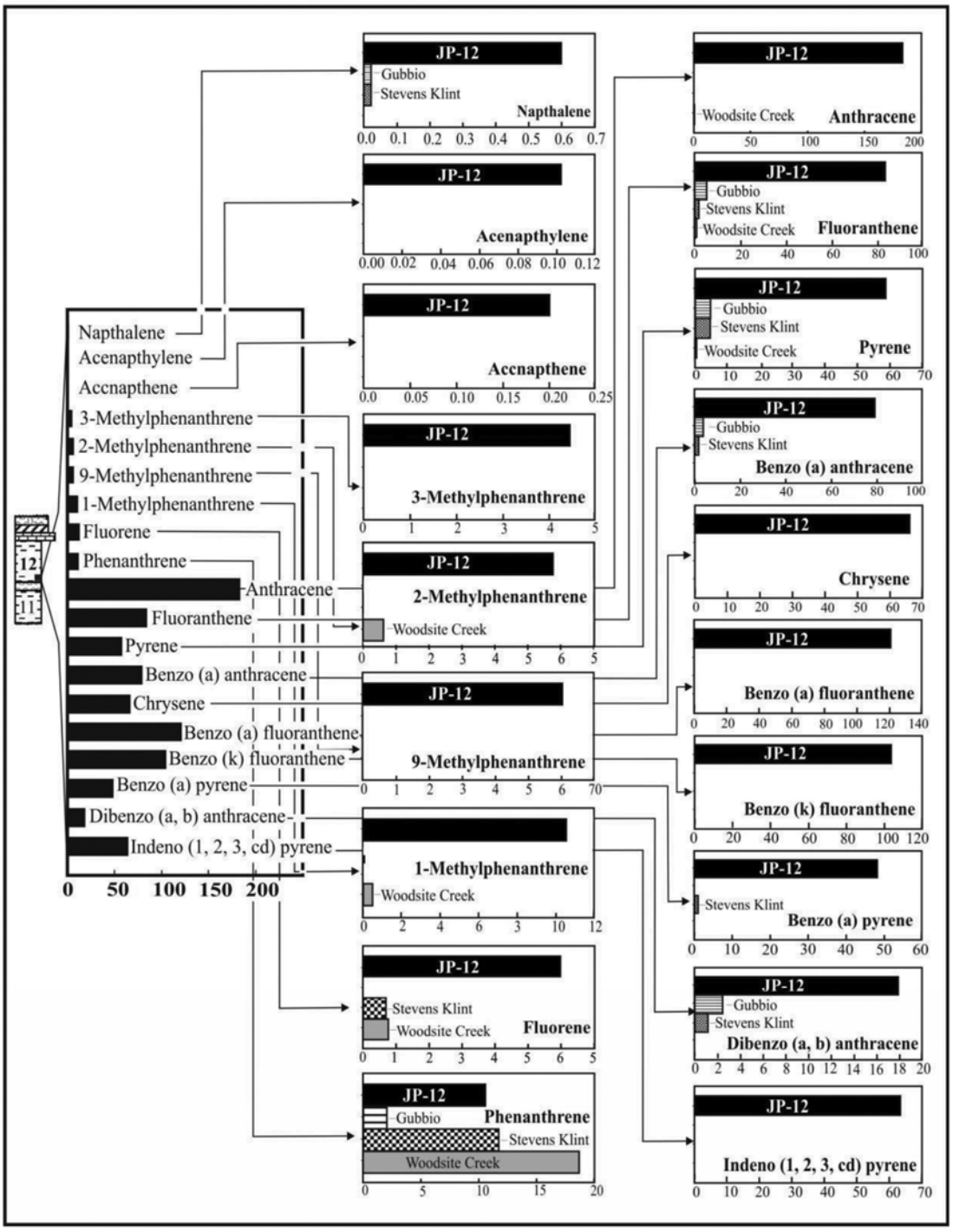

Figure 6. PAH compound data with respect to biozone CF3 showing excursions with respect to combustion marker PAH compounds and their comparison with the K/T boundary sections of Stevns Klint (Denmark), Gubbio (Italy) and Woodside Creek (New Zealand), representing K/Pg transition layer.

and preceded the K/Pg boundary layer. The yellow clay stone layer containing anomalous concentration of some platinum group elements (PGE) and concentration of microspherules in biozone CF2 succeeded the fire event, but also happened prior to the biostratigraphically detected K/Pg boundary layer. Among the four biozones (CF4, CF3, CF2 and CF1 in ascending order) in the upper Maastrichtian part of the upper Maastrichtian–lower Danian transition section, the two major phases of Deccan eruptions were earlier calibrated[13] with CF4 and CF2. Incidence of coal in CF4 might have developed due to induced heat of the eruption. The PGE concentration could

be linked with the second phase of eruption during CF2. Minor eruption might have occurred during CF3 to supply heat for fire. Alternately, the Abor Volcanics that erupted in two episodes – Permian and Paleocene–Eocene might have provided the heat for fire during late Maastrichtian biozone CF3 (ref. 29). Complex organic molecules-derived LMW PAH compounds resulted from the sudden increase in temperature, but at low pressures. Its excursion (sample JP-13 in biozone CF2) corresponds to 65.45–65.3 Ma, coeval with the most vigorous second episode of Deccan volcanic eruption that occurred during the deposition of the greenish-yellow layer in biozone CF2 at 65.4–65.2 Ma (ref. 37) and also marked by the first appearance of *Plummerita hantkeninoides*. Massive greenish-yellow (with thin lamination of) silty layer (sample JP-13) lies within the grey calcareous marl (20 cm thick), which also represents Au, Pt and Pd excursions in biozone CF2, just below the K/Pg boundary layer[13]. The biozone CF1 represents a regressive regime. General absence of *Psedutexularia elegans* in biozone CF1 is also noticed, indicating that the species were unable to sustain in the cold sea water. The size reduction of *P. elegans* is possibly due to stressful environmental conditions – warming in the climate, acid rain and CO_2 emissions related to Deccan volcanism and sea-level changes or sea replacement of Tethys by Indo-Pacific Ocean, or by local tectonic changes[38].

However, the presence of abnormally high amount of combustion-derived PAH compounds in the yellowish-brown clay layer of biozone CF3 (sample JP-12) corresponds to 66.83–65.45 Ma coinciding with the Ce anomaly layer[11], but preceeded by the planktonic foraminiferal break and PGE anomaly-bearing layer, lying between biozones P0 and CF2 (refs 12, 13). The collision of the Indian plate with the Burmese–Indonesian plates along the Assam–Arakan–Andaman mobile belt[39] and its collision with the Eurasian plate (66 Ma), possibly occurred during the sedimentation of biozone CF3 and the pulses of these movements disturbed the sea shelf. Perhaps, extrusion of Abor Volcanics (erupted in two episodes – Permian and Paleocene–Eocene)[29] across the K/Pg boundary[13] marginally increased the temperature of the oceanic water, but the rise in temperature was inadequate for the survival of *P. elegans.* Consequently, the rise in the level of shelf waters was explained due to plate collision and despite attendant transgression, *P. elegans* did not appear[13]. However, 66 Ma age is assigned for the K/Pg boundary[35]. Of late, an absolute age for the K/Pg boundary has been assigned as 66.043 ± 0.043 Ma (ref. 40). Therefore, deposition of 1–2 mm thick, yellowish-brown (smooth, with conchoidal fracture + pyrite nodules and micro-spherules), organic-rich clay layer (with decrease in carbonate content (2.43%)) which lies at the contact between the silty mudstone and grey calcareous shale located in biozone CF3 (sample JP-12) of this succession coincides with the first appearance of *Pseudoguembelina hariaensis* representing an age of 66.83–65.45 Ma and is also related to India's collision with Eurasia and Burma and extrusion of Abor Volcanics[28]. The lateral continuity of this layer is limited and persists for a short distance; however, discrete patches of yellowish-brown clay layer exist in the underlying and overlying layers. Therefore, foraminiferal break[12], which occurs at the contact between biozones CF1 and P0, and PGE anomaly layer[13] that occurs in biozone CF2 are related to the extinction of *P. hantkeninoides* events and presence of abnormally high concentrations of Au, Pt and Pd anomalies in biozone CF2. However, deposition of Ce (ref. 14) and organic anomaly-bearing layer (sample JP-12 in biozone CF3) is preceded by shaly marlite (sample JP-14) and greenish-yellow coloured (sample JP-13) layer, and is related to K/Pg boundary event.

Biostratigraphically well-constrained K/Pg section along the Um Sohryngkew river, Meghalaya represents distribution of several types of PAH compounds. Anomalously high concentration of these compounds was detected in the late Maastrichtian biozone CF3, and based on pyrolitic signatures the cause is considered as regional terrestrial fire. This regional incidence might have caused distress to biota during CF3. The distribution of PAH compounds also endorses succeeding events like anomalous concentration of PGE and concentration of spherules during biozone CF2 (ref. 13), which advent before the K/Pg boundary.

1. Riboulleau, A., Schnyder, J., Riquier, L., Lefebvre, V., Baudin, F. and Deconinck, J. F., Environmental change during the Early Cretaceous in the Purbeck-type Durlston Bay section (Dorset, Southern England): a biomarker approach. *Org. Geochem.*, 2007, **38**, 1804–1823.
2. Shrivastava, J. P. and Ahmad, M., Compositional studies on organic matter from iridium-enriched Anjar intertrappean sediments: Deccan volcanism and palaeoenvironmental implications during the Cretaceous/Tertiary boundary. *J. Iberian Geol.*, 2004, **31**, 167–177.
3. Tschudy, R. H., Pillmore, C. L., Orth, C. J., Gilmore, J. S. and Knight, J. D., Disruption of the terrestrial plant ecosystem at the Cretaceous–Tertiary boundary, Western Interior. *Science*, 1984, **225**, 1030–1032.
4. Wolbach, W. S., Gilmour, I. and Anders, E., Major wildfires at the K–T boundary. *Geol. Soc. Am. Spec. Pap.*, 1990, **247**, 391–400.
5. Heymann, D., Yancey, T. E., Wolbach, W. S., Thiemens, M. H., Johnson, E. A., Roach, D. and Moecker, S., Geochemical markers of the Cretaceous–Tertiary boundary event at Brazos River, Texas, USA. *Geochim. Cosmochim. Acta*, 1998, **62**, 173–181.
6. Arinobu, T., Ishiwatari, R., Kaiho, K. and Lamolda, M. A., Spike of pyrosynthetic polycyclic hydrocarbons associated with an abrupt decrease in $\delta^{13}C$ of a terrestrial biomarker at the Cretaceous–Tertiary boundary at Caravaca, Spain. *Geology*, 1999, **27**, 723–726.
7. Nagappa, Y., Foraminiferal biostratigraphy of the Cretaceous–Eocene succession in the India–Pakistan–Burma region. *Micropaleontology*, 1959, **5**, 145–192.
8. Shrivastava, J. P., Salil, M. S. and Pattanayak, S. K., Clay mineralogy of Ir-bearing intertrappean, Kutch, Gujrat, India: inference on paleoenvironment. *J. Geol. Soc. India*, 2000, **55**, 197–206.

9. Shrivastava, J. P. and Ahmad, M., Compositional studies on illite–smectite from iridium enriched and other infra (Lametas)/intertrappean sediments from Deccan Traps. *Indian J. Geochem.*, 2005, **20**, 121–142.
10. Shrivastava, J. P. and Ahmad, M., Trace element compositions of iridium-enriched illite–smectite assemblages from a K/Pg boundary section in the Anjar area of the Deccan volcanic province: palaeoenvironmental implications. *Cretaceous Res.*, 2008, **29**, 592–602.
11. Pal, S., Srivastava, S. and Shrivastava, J. P., Mineral chemistry of clays associated with the Jhilmili Intertrappean Bed in the Eastern Deccan volcanic province: palaeoenvironmental inferences and KTB transition. *J. Geol. Soc. India*, 2013, **82**, 38–52.
12. Mukhopadhyay, S. K., Planktonic foraminiferal succession in late Cretaceous to early Palaeocene strata in Meghalaya, India. *Lethaia*, 2008, **41**, 71–84.
13. Mukhopadhyay, S. K., Convener's report for 2008 on the progress of work in the IGCP Project 507, on 'Palaeoclimate in Asia during the Cretaceous: their variations, causes, and biotic and environmental responses'. *IGCP India Newsl.*, 2009, **29**, 11–13.
14. Shrivastava, J. P., Mukhopadhyay, S. K. and Pal, S., Chemico-mineralogical attributes of clays from the late Cretaceous early Palaeogene succession of the Um Sohryngkew river section of Meghalaya, India: palaeoenvironmental inferences and the K/Pg boundary. *Cretaceous Res.*, 2013, **45**, 247–257.
15. Gill, R., *Modern Analytical Geochemistry. An Introduction to Quantitative Chemical Analysis Techniques for Earth, Environmental and Material Scientists*, Adision Wesley Longman Ltd, Edinburgh, 1997, p. 317.
16. Arinobu, T., Ishiwatari, R., Kaiho, K., Lamolda, M. A. and Seno, H., Abrupt massive influx of Terrestrial biomarkers into the marine environment at the Cretaceous–Tertiary boundary, Caravaca, Spain. *Palaeogeogr. Palaeoclimatol. Palaeoecol.*, 2005, **224**, 108–116.
17. Vinas, L., Franco, M. A. and Gonzalez, J. J., Polycyclic aromatic hydrocarbon composition of sediments in the Ria de Vigo (NW Spain). *Arch. Environ. Contam. Toxicol*, 2009, **57**, 42.
18. Budzinski, H., Jones, I., Bellocq, J., Pierrard, C. and Garrigues, P., Evaluation of sediment contamination by polycyclic aromatic hydrocarbons in the sediment of the Georges River estuary. *Mar. Chem.*, 1997, **58**, 85–97.
19. Baumard, P., Budzinski, H., Garrigues, P., Dizer, H. and Hansen, P. D., Polycyclic aromatic hydrocarbons in recent sediments and mussels (*Mytilus edulis*) from the western Baltic Sea: occurrence bioavailability and seasonal variations. *Mar. Environ. Res.*, 1999, **47**, 17–47.
20. Wang, Z., Fingas, M. and Page, D. S., Oil spill identification. *J. Chromat.*, 1999, **843**, 369–411.
21. Yunker, M. B. and Macdonald R. W., Composition and origin of polycyclic aromatic hydrocarbons in the Mackenzie River and on the Beaufort Sea Shelf. *Arctic*, 1995, **48**(2), 118–129.
22. Killops, S. D. and Massoud, M. S., Polycyclic aromatic hydrocarbons of pyrolytic origin in ancient sediments: evidence for Jurassic vegetation fires. *Org. Geochem.*, 1992, **18**, 1–7.
23. Jiang, C., Alexander, R., Kagi, R. I. and Murray, A. P., Polycyclic aromatic hydrocarbons in ancient sediments and their relationships to palaeoclimate. *Org. Geochem.*, 1998, **29**, 1721–1735.
24. Collins, J. F., Brown, J. P., Alexeff, G. V. and Salmon, A. G., Potency equivalency factors for some polycyclic aromatic hydrocarbons and polycyclic aromatic hydrocarbon derivatives. *Regul. Toxicol. Pharmacol.*, 1998, **28**(1), 45–54.
25. Benlahcen, K. T., Chaoui, A., Budzinski, H., Bellocq, J. and Garrigues, P. H., Distribution and sources of polycyclic aromatic hydrocarbons in some Mediterranean coastal sediments. *Mar. Pollut. Bull.*, 1997, **34**(5), 298–305.
26. Venkatesan, M. I. and Dahl, J., Organic geochemical evidence for global fires at the Cretaceous/Tertiary boundary. *Nature*, 1989, **338**, 57–60.
27. Laflamme, R. E. and Hites, R. A., The global distribution of polycyclic aromatic hydrocarbons in recent sediments. *Geochim. Cosmochim. Acta*, 1978, **42**, 289–303.
28. Shankar, R., Kumar, G. and Saxena, S. P., Stratigraphy and sedimentation in Himalaya: a reappraisal. *Geol. Surv. India Spec. Publ.*, 1989, **26**, 1–60.
29. Acharya, S. K. and Puspendu, S., Age and tectono-magmatic setting of Abor Volcanics, Siang window, Eastern Himalayan syntaxial area, India. *J. Appl. Geochem.*, 2013, **15**, 170–192.
30. Beck, R. A. *et al.*, Stratigraphic evidence for an early collision between northwest India and Asia. *Nature*, 1995, **373**, 305–327.
31. Robertson, D. S., McKenna, M. C., Toon, O. B., Hope, S. and Lillegraven, J. A., Comment on Fireball passes and nothing burns – the role of thermal radiation in the Cretaceous–Tertiary event: evidence from the charcoal record on North America. Geology Online Forum, 2004, 10.
32. Finkelstein, D. B., Pratt, L. M., Curtin, T. M. and Brassell, S. C., Wildfires and seasonal aridity recorded in Late Cretaceous strata from south-eastern Arizona, USA. *Sedimentology*, 2005, **52**, 587–599.
33. Belcher, C. M., Finch, P., Collinson, M. E., Scott, A. C. and Grassineau, N. V., Geochemical evidence for combustion of hydrocarbons during the K–T impact event. *Proc. Natl. Acad. Sci. USA*, 2009, **106**, 4112–4117.
34. Chenet, A. L. *et al.*, Determination of rapid Deccan eruptions across the Cretaceous–Tertiary boundary using paleomagnetic secular variation: 2. Constraints from analysis of eight new sections and synthesis for a 3500-m-thick composite section. *J. Geophys. Res.*, 2009, **114**, B06103 (1–38).
35. Gradstein, F. M., Ogg, J. G., Schmitz, M. and Ogg, G., *The Geologic Time Scale 2012*, Elsevier, 2012, p. 1144.
36. Kruge, M. A., Stankiewicz, B. A., Crelling, J. C., Montanari, A. and Bensley, D. F., Fossil charcoal in Cretaceous–Tertiary boundary strata: evidence for catastrophic firestorm and megawave. *Geochim. Cosmochim. Acta*, 1994, **58**, 1393–1397.
37. Hoffman, C., Feraud, G. and Courtillot, V., $^{40}Ar/^{39}Ar$ dating of mineral separates and whole rock from the Western Ghat lava pile: further constraints on duration and age of Deccan Traps. *Earth Planet. Sci. Lett.*, 2000, **180**, 13–27.
38. Mukhopadhyay, S. K., Morphogroups and small sized tests in *Pseudotextularia elegans* (Rzehak) from the Late Maastrichtian succession of Meghalaya, India as indicators of biotic response to paleoenvironmental stress. *J. Asian Earth Sci.*, 2012, **48**, 111–124.
39. Wakita, K. and Metcalfe, I., Ocean plate stratigraphy in East and Southeast Asia. *J. Asian Earth Sci.*, 2005, **24**, 679–702.
40. Paul, R. R. *et al.*, Time scale of critical events around Cretaceous–Paleogene boundary. *Science*, 2013, **339**, 684–687.

ACKNOWLEDGEMENTS. We thank Dr Aninda Mazumdar and Dr B. G. Naik (NIO, Goa) for GC-MS analysis of samples. S.P. and J.P.S. thank CSIR, New Delhi for financial support [Project Grant No. 24 (0315)/11/EMR-II]. J.P.S. and S.K.S. thank IGCP for funds (IGCP Project Grant-507) to carry out field work.

Received 18 October 2014; revised accepted 26 May 2015

doi: 10.18520/v109/i6/1140-1150